Diabetes, Metabolic Syndrome and Obesity

Dovepress

open access to scientific and medical research

Open Access Full Text Article

ORIGINAL RESEARCH

Hepatocyte-Specific *Yap1* Knockout Maintained the Liver Homeostasis of Lipid Metabolism in Mice

Caige Li[1,2], Yu Xue[1], Yiwei Liu[1], Kangning Zheng[1], Yuting Gao[1,3], Yi Gong[1], Junlan Lu[1], Yuman Zhang[1], Jingmin Ji[1], Zhiqin Zhang[1], Xinli Shi[1]

[1]Department of Pathobiology and Immunology, Hebei University of Chinese Medicine, Shijiazhuang, Hebei, People's Republic of China; [2]Department of Endocrinology, The Second Hospital of Hebei Medical University, Shijiazhuang, Hebei, People's Republic of China; [3]School of Basic Medical Sciences, Shanxi University of Chinese Medicine, Jinzhong, Shanxi, People's Republic of China

Correspondence: Xinli Shi, Department of Pathobiology and Immunology, Hebei University of Chinese Medicine, 3 Xingyuan Road, Shijiazhuang, Hebei, 050200, People's Republic of China, Tel +86-0311-89926237, Email sxlsunshine@sina.com

Introduction: Yes-associated protein 1 (YAP1) is a crucial molecule in the Hippo pathway. The impact of hepatocyte-specific *Yap1* knockout ($Yap1^{LKO}$) on hepatic lipid droplets (LD) and pePLIN2 in metabolic fatty liver has not been reported. This study aims to explore whether $Yap1^{LKO}$ could offer a protective effect in a liver injury model.

Methods: Three-week-old $Yap1^{LKO}$ and $Yap1^{Flox}$ mice were given aristolochic acid I (AAI) combined carbon tetrachloride (CCL_4) establish liver injury model. Eight-week-old $Yap1^{LKO}$ and $Yap1^{Flox}$ mice were fed with a high-fat diet for 18 weeks to establish obesity-related liver injury model. Further biochemical, histomorphological, immunohistochemical, and lipidomic analyses were performed on serum and liver tissues of these mice to elucidate the effects of hepatocyte-specific *Yap1* knockout on hepatic lipid metabolism.

Results: $Yap1^{LKO}$ reduced triglyceride (TG) content and PLIN2 expression level in the liver during the intervention of AAI combined CCl_4. Moreover, $Yap1^{LKO}$ improved lipid metabolism homeostasis in the liver by increasing the beneficial lipid molecules and reducing the harmful lipid molecules through lipidomics. Finally, $Yap1^{LKO}$ reduced TG content in the serum and liver, hepatic vacuolar degeneration, and hepatic PLIN2 expression level in mice fed with a high-fat diet (HFD).

Conclusion: $Yap1^{LKO}$ is protective in regulating liver and blood TG when induced with toxic substances AAI combined CCl_4 and a high-fat diet.

Keywords: yes-associated protein, hepatocyte-specific *Yap1* knockout, perilipin-2, lipidomic, triglyceride

Introduction

Yes-associated protein 1 (YAP1) was a key molecule of the Hippo pathway.[1] The Hippo pathway has emerged as an evolutionarily conserved master regulator of organ size and tissue growth.[2] Most studies on YAP1 focused on tumor-related diseases.[3] YAP1 is a nuclear co-factor of sterol regulatory element binding proteins (SREBPs) and the Hippo pathway negatively affects hepatocyte lipogenesis by inhibiting the function of YAP-SREBP complexes.[4] Adipocyte-specific YAP deficiency increased adipocyte death during obesity.[5] Our previous studies found that YAP1 knockdown/knockout reduced lipid droplet (LD) deposition and triglyceride (TG) content in liver tumor cells.[6] TG was one of the main components of LD.[7] YAP increased in non-alcoholic fatty liver disease (NAFLD), and mainly localized in the nuclei of hepatocytes, perivascular cells and bile duct cells. YAP accumulation correlated with the severity of hepatocyte injury.[8] Perilipin-2 (PLIN2) overexpression induced LD accumulation, and PLIN2 ablation reduced LD.[9] The effect of hepatocyte-specific *Yap1* knockout ($Yap1^{LKO}$) on hepatic lipid droplets and PLIN2 in metabolic fatty liver has not been reported.

Received: 12 June 2024
Accepted: 16 August 2024
Published: 27 August 2024

Aristolochic acid (AA), a nitrophenanthrene carboxylic acid compound, had anti-tumor, anti-inflammatory, analgesic and other pharmacological effects. Before stricter regulations in 2003, more than 100 million people in China used Chinese herbs containing AA.[10] Aristolochic acid I (AAI) was considered the main toxic chemical of aristolochic.[11] Metabolomics analysis revealed the lipid abnormalities in AAI-induced nephropathy.[12] Some studies have shown that in human hepatocyte samples treated with AA, significant changes have occurred in metabolic substances, mainly the increase of some harmful lipids.[13] Carbon tetrachloride (CCL_4) is a classic chemical agent that causes liver injury and enhances hepatotoxicity by inducing liver injury, compensatory proliferation, inflammation, and fibrosis.[14,15] A study showed that the liver injury was obvious after CCL_4 treatment, and the levels of phosphatidylcholine (PC) and phosphatidylethanolamine (PE) were significantly decreased in the liver and serum.[16] Low-dose AAI+CCL_4 induced the primary hepatocellular carcinoma.[17]

Lipids, including fatty acids (FAs), glycerols, phospholipids, and sphingolipids, related to tumor biology. Phospholipids, including sphingolipids and phospholipids, were the main structural molecules of cell membrane and played an essential role in maintaining cell membranes barrier function and fluidity.[18] Lipidomics has recently become a powerful tool for evaluating drug safety.[19] It quantitatively determined lipids in tissues or organisms.[20] However, no study has been reported on hepatocyte-specific *Yap1* knockout regulating LD deposition and lipidomics. Therefore, exploring the effects of $Yap1^{LKO}$ on liver lipidomics will elucidate the role of hepatocyte YAP1 in liver lipid metabolism.

Our previous research found that YAP1 was highly expressed in livers with metabolic dysfunction-associated fatty liver disease (MAFLD), and $Yap1^{LKO}$ reduced LD deposition in mice.[21] In this study, we compared the difference in lipid biomarkers between $Yap1^{LKO}$ and $Yap1^{Flox}$ mice, and identified some lipid markers in the liver. We found that $Yap1^{LKO}$ reduced TG content and maintained lipid metabolism homeostasis in the liver. It provided a basis for further exploring the role of YAP1 in liver protection.

Materials and Methods

Animal Model

The C57BL/6 mice used in all experiments were obtained and identified from the Guangzhou Cyagen Biosciences (Guangzhou, China). Animals were housed at a constant temperature and a 12h light/dark cycle with standard food and free access to water.

Hepatocyte-specific *Yap1* knockout mice (marked as $Yap1^{LKO}$ mice) were constructed and identified by Cyagen Biosciences (Guangzhou, China); the schematic illustration of the multiplication of mice and identification bands is shown in (Figure 1A). We used $Yap1^{Flox}$ as the control. Based on previous research, we administered AAI (Med et al, HYW00035460) by intraperitoneal injection in the mice at 2.5 mg/kg body weight for 14 d. Moreover, we employed AAI-administered mice exposed to 0.5 mL/kg of CCL_4. Three-week-old $Yap1^{LKO}$ and $Yap1^{Flox}$ male mice were intraperitoneally injected with aristolochic acid I (2.5 mg/kg/ day) for 14 d. Mice were injected with carbon tetrachloride (0.5 mL/kg/ week) once a week for ten consecutive times starting at 5 weeks of age (Figure 1B). At 26 weeks of age, mice were anesthetized, and sacrificed by blood sampling and livers were rapidly harvested for further study.

The metabolic dysfunction-associated fatty liver disease was induced in the mice by feeding them a high-fat diet (HFD, 40% high-fat purified feed and 0.15% cholesterol). We used male $Yap1^{LKO}$ and $Yap1^{Flox,}$ aged 7–8 weeks (23±2g). The mice were each divided into two groups (n = 8). The normal diet (ND) group received an ND and water for 18 weeks. The HFD group was given an HFD for 18 weeks. All the animals were sacrificed, and the livers were removed, weighed, and fixed in 4% paraformaldehyde and embedded in paraffin wax.

All experimental procedures described in the present work were performed according to the Provision and General Recommendation of the Chinese Laboratory Association and were fully compliant with the Institutional Animal Care and Use Committee of the Hebei University of Chinese Medicine (No. DWLL2021095).

Hematoxylin-Eosin Staining

All aliquots of organs were quickly removed and rinsed with cold phosphate-buffered saline. Then, liver tissues were fixed by 4% paraformaldehyde solution, dehydrated, embedded in paraffin, prepared at 4 μm thickness, and stained with H&E. Finally, we observed and described in a panoramic scanner for histopathological examination (Motic DSAssistant).

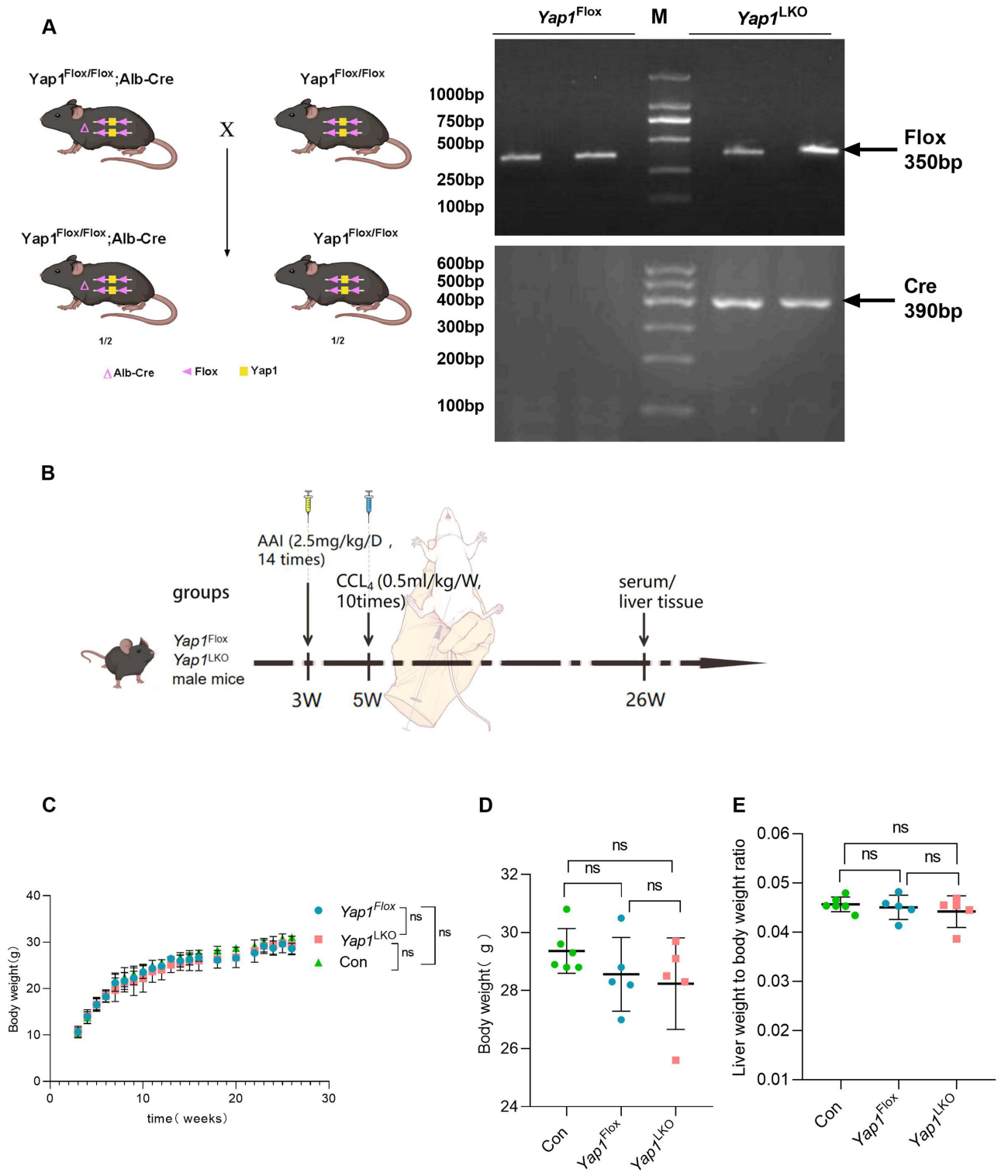

Figure 1 Distribution and modeling of hepatocyte-specific *Yap1* knockout mice. (**A**) Distribution map and PCR identification strip of hepatocyte-specific *Yap1* knockout mice. (**B**) AAI+CCL_4 model diagram. (**C**) Dynamic observation weight in mice, no statistical difference between the three groups (n≥5). (**D**) Body weight of the 26-week-old mice was not statistically different among the three groups (n≥5). (**E**) The liver weight to body weight was not statistically different among the three groups (n≥5).

Immunohistochemistry

Paraffin-embedded liver biopsies were cut into 4 μm serial sections. The slices were placed in citrate buffer (pH = 6.0) in a pressure cooker for 3 min. They were rinsed and washed with PBS buffer and blocked with normal goat serum working

https://doi.org/10.2147/DMSO.S472778 DovePress

solution. Appropriate amount of primary anti-rabbit PLIN2 (15294-1-AP, Proteintech, 1:275), anti-rabbit YAP1(#14704T, CST, 1:200) was added, and the samples were incubated in a refrigerator overnight. Rinsed with PBS buffer, incubated with horseradish enzyme-labeled streptolysin working solution at room temperature, rinsed with PBS buffer, added with newly prepared DAB color solution, stained with hematoxylin, dehydrated and transparent with ethanol and xylene. All the images were acquired a panoramic scanner (Motic DSAssistant).

Biochemical Analysis

Biochemical reagents bought from Shanghai Zhicheng biological technology co., LTD. The levels of serum biochemistry, including alanine aminotransferase (ALT, ZCDECT016), aspartate aminotransferase (AST, ZCJANU014), glucose (GLU, ZCNOVT028), total bilirubin (TBIL, ZCDECT006), triglyceride (TG, ZCOCTT006), Total cholesterol (CHO, ZCDECT025), high-density lipoprotein (HDLC, ZCMAYU004), light-density lipoprotein (LDLC, ZCDECT002) were detected by the Beckman automatic biochemical analyzer AU680 (Backman, USA).

Metabolite Extraction

Transfer 100 mg of each sample into 2 mL centrifuge tubes, add 750 μL of Chloroform methanol mixed solution (2:1) (pre-cooled at −20°C), vortex for 30s. Add 2 steel balls, put them into the tissue grinder and grind for 90s at 55 Hz. Put on the ice for 40 min, add 190 μL H_2O, vortex for 30s, and still put on the ice for 10 min; Centrifuged at 12,000 rpm for 5 min at room temperature and transfer 300 μL lower layer fluid into a new centrifuge tube. Add 500 μL of Chloroform methanol mixed solution (2:1) (pre-cooled at −20°C), vortex for 30s. Centrifuged at 12,000 rpm for 5 min at room temperature and transfer 400 μL lower layer fluid into the same centrifuge tube above. Samples were concentrated to dry in vacuum. Dissolve samples with 200 μL isopropanol, and the supernatant was filtered through 0.22 μm membrane to obtain the prepared samples for liquid chromatography-mass spectrometry (LC-MS). Take 20 μL from each sample to the quality control (QC) samples. (These QC samples were used to monitor deviations of the analytical results from these pool mixtures and compare them to the errors caused by the analytical instrument itself). Use the samples for LC-MS detection.[16]

Liquid Chromatography Method

Chromatographic separation was performed on Thermo Ultimate 3000 system equipped with an ACQUITY UPLC® BEH C18 (100 × 2.1 mm, 1.7 μm, Waters) column maintained at 50°C. The autosampler temperature was 8°C. Gradient elution of analytes was carried out with acetonitrile:water = 60:40 (0.1% formic acid +10 mM ammonium formate) and isopropanol:acetonitrile = 90:10 (0.1% formic acid+10mM ammonium formate) at a flow rate of 0.25 mL/min. After equilibration, injection of 2 μL of each sample was performed. An increasing linear gradient of solvent C (v/v) was used as follows: 0–5 min, 70–57% C; 5–5.1 min, 57%–50% C; 5.1–14 min, 50%–30% C; 14–14.1 min, 30% C; 14.1–21 min, 30%–1% C; 21–24min, 1% C; 24–24.1 min, 1%–70% C; 24.1–28 min, 70% C[16] (Suzhou Panomic Biomedical Technology Co., LTD. Project Number: HT2021042826007).

Mass Spectrometry Method

The ESI-MSn experiments were conducted on the Thermo Q Exactive Plus mass spectrometer with the spray voltage of 3.5 kV and −2.5 kV in positive and negative modes, respectively. The auxiliary gas and sheath gas were set at 10 and 30 arbitrary units, respectively. The temperature of capillary was 325°C. The Orbitrap analyzer had a scan mass range of m/z 150–2000 for full scan at a mass resolution of 35,000. Data dependent acquisition (DDA) MS/MS experiments were conducted with HCD scan. The normalized collision energy was 30 eV. A dynamic elimination method was used to remove some unnecessary information in MS/MS spectra[16] (Suzhou Panomic Biomedical Technology Co., LTD. Project Number: HT2021042826007).

Statistical Analysis

All statistical tests were performed using SPSS23.0 statistics software (IBM Corp). All in vitro experiments were repeated at least 3 times, and at least three samples were taken at a time. A *t*-test was used to determine the statistical

significance of the comparison between the two groups. When more than two groups were compared, one-way ANOVA was used for comparison. $P<0.05$ was considered to indicate a statistically significant difference. Parletto (Par) conversion processing was performed on the data before multivariate statistical analysis in this lipidomics. The multivariate statistical analysis (R language ropls package) methods used in this analysis are as follows: Principal Component Analysis (PCA), Partial Least Squares Discriminant Analysis (PLS-DA), Orthogonal Partial Least Squares Discriminant Analysis (OPLS-DA).

Results

Liver Lipid Droplets Deposition was Decreased in *Yap1*^{LKO} Mice

The schematic illustration of the multiplication of *Yap1*^{LKO} mice and identification bands is shown in Figure 1A. In this study, the model diagram of animal grouping and treatment is shown in Figure 1B. The weight changes of mice were observed dynamically, and there was no difference in weight among the three groups (Figure 1C). The body weight and the liver index were no different in the three groups (Figure 1D and E). No tumor cells were found in the livers of both *Yap1*^{LKO} and *Yap1*^{Flox} groups, and only white particles were seen on the liver surface, which were found to be encapsulated by inflammatory cells by H&E staining (Figure 2). After AAI+CCL_4 was induced, liver LD deposition increased, while *Yap1*^{LKO} group had higher liver density and less liver LD deposition than the *Yap1*^{Flox} group (Figure 3A). These results showed that treatment of 3-week-old mice with AAI did not induce liver tumors. *Yap1*^{LKO} did not affect mice's body weight and liver index but reduced liver LD deposition.

The Level of Triglyceride was Decreased in *Yap1*^{LKO} Mice

Subsequently, we carried out biochemical tests on the serum respectively. Safety indexes, such as ALT, AST, and TBIL, showed no changes in serum in *Yap1*^{LKO} group compared with *Yap1*^{Flox} group (Figure 3B). The content of cholesterol and glucose from the two groups was not statistically difference in serum. However, triglyceride (TG) content decreased in *Yap1*^{LKO} group compared with *Yap1*^{Flox} group in the serum (Figure 3C). These results showed that *Yap1*^{LKO} mainly affected the TG content in the serum induced by AAI +CCL_4.

Yap1^{LKO} Improved Lipid Disorder Induced by AAI + CCL_4

To investigate changes to lipid metabolism, we performed liver lipidomic experiments on the models of *Yap1*^{LKO} and *Yap1*^{Flox} mice after AAI combined with CCL_4 intervention. The principal component analysis (PCA) score plot clearly distinguished between *Yap1*^{LKO} and *Yap1*^{Flox} group (Figure 4A). The model predicted well and exhibited an empirical R2X of 0.619 in the permutation test. This test suggested that hepatocyte-specific *Yap1* knockout changed hepatic lipid metabolism abnormalities by AAI combined with CCL_4. Partial least-squares discriminant analysis (PLS-DA) was performed to evaluate the lipid profile alterations related to *Yap1*^{LKO} and *Yap1*^{Flox} group (Figure 4B). The model predicted well (R2Y=0.85 and R2X=0.549) and exhibiting an empirical 0.468 in the permutation test. Orthogonal Partial Least Squares Discriminant Analysis (OPLS-DA) was performed to evaluate the lipid profile alterations related to *Yap1*^{LKO} and *Yap1*^{Flox} group (Figure 4C). The model predicted well (R2Y=0.85 and R2X=0.549), exhibiting an empirical R2 of 0.565 in the permutation test. A total of 3806 lipid species and 67 lipid classes were identified by the lipidomic analysis (Table S1). OPLS-DA analysis showed that *Yap1*^{LKO} group had a more significant change in liver lipid metabolites, including TG (16:0_18:2_20:4), TG (18:1_18:2_20:4), PE (19:0e), MePC (33:1), MePC (35:3), TG (18:0_18:1_18:2) and TG (18:1_18:2_18:2) (Figure 4D). Classification analysis showed that glycerolipids and phospholipids were the most abundant changed lipid categories which have been identified so far, followed by saccharolipids, sphingolipids, sterol lipids, fatty acyl, and prenol lipids, compared with the *Yap1*^{Flox} group (Figure 4E). To further illustrate the relationship between the number of changed lipids in each lipid subclass and the number of detected lipids, the percentage of 7 lipids was plotted in the detected lipids (Figure 4F). Although the changed numbers of some lipids were small, they account for a high proportion of detected lipids, indicating that these lipids also changed obviously. These results suggested that *Yap1*^{LKO} improved liver lipid metabolism disorder induced by AAI combined with CCL_4.

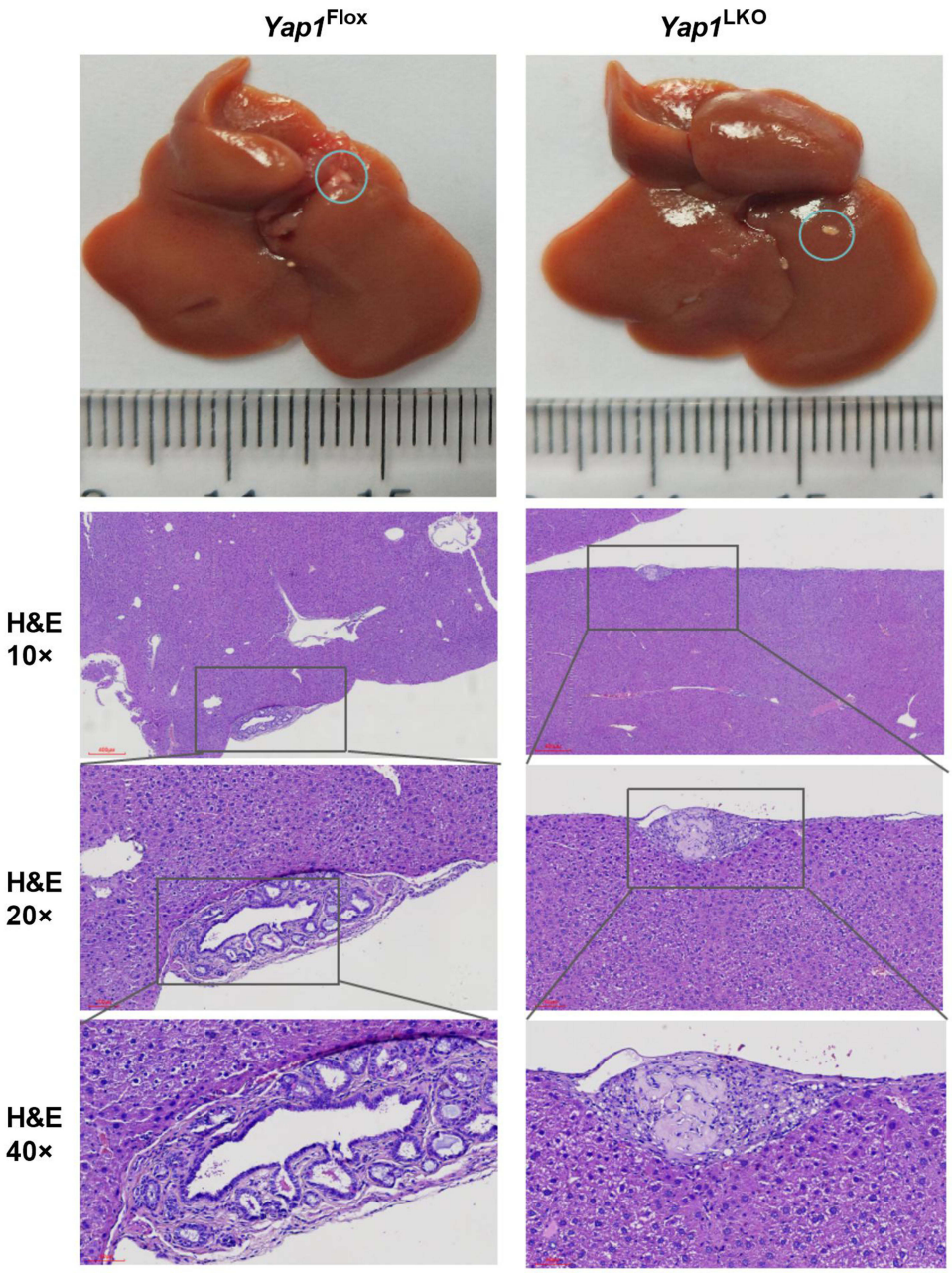

Figure 2 Liver appearance and pathology of mice aged 26 weeks after AAI combined CCL_4 intervention. No tumor cells were found in the livers of both *Yap1*^{LKO} and *Yap1*^{Flox} groups, and only white particles were seen on the liver surface, which were found to be encapsulated by inflammatory cells.

Yap1^{LKO} Changed 7 Different Lipid Subclasses

Since liver lipid levels were significantly altered on *Yap1*^{LKO}, further analyses were performed to examine lipid composition. Among the identified subclasses, 135 lipid molecules changed significantly and belonged to 7 different lipid subclasses. Over one-third of changed lipids belong to phospholipids, including lysophosphatidylcholine (LPC), lysophosphatidylethanolamine (LPE), phosphatidylcholine (PC), phosphatidylethanolamine (PE), phosphatidylserine (PS), phosphatidylglycerol (PG) and phosphatidylinositol (PI/PIP). The second lipids belong to glycerolipids, including diglyceride (DG) and TG; prenol lipids, including coenzyme (Co); fatty acyls, including fatty acid (FA) and N-acylethanolamine (AEA); sterol lipids, including cholesterol ester (ChE), campesterol ester (CmE), zymosterol ester (ZYE); sphingolipids, including sphingomyelin (SM), simple glc series ceramides (Hex1Cer) and simple GLC series

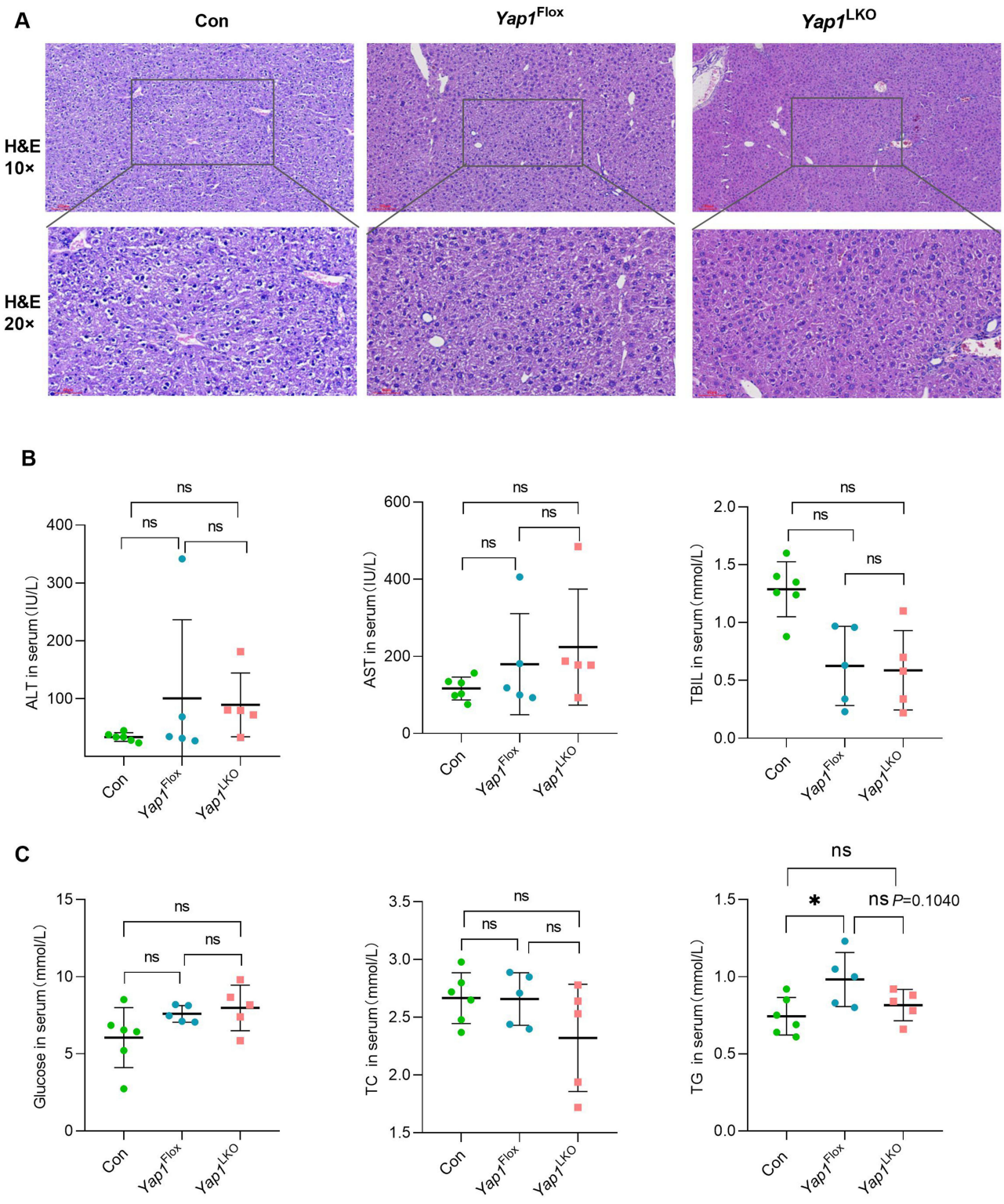

Figure 3 Effects of hepatocyte-specific *Yap1* knockout on hepatic histology and serum biochemical indexes. (**A**) Effects of hepatocyte-specific *Yap1* knockout on hepatic histology on lipids accumulation. (**B**) Serum biochemical safety index ALT, AST, and TBIL are not statistically different among the three groups. (**C**) Serum metabolic index cholesterol and glucose are not statistically different among the three groups. The serum triglyceride level of the *Yap1*^{LKO} group had a decreasing trend compared with the *Yap1*^{Flox} group. *P<0.05. n≥5.

https://doi.org/10.2147/DMSO.S472778 DovePress

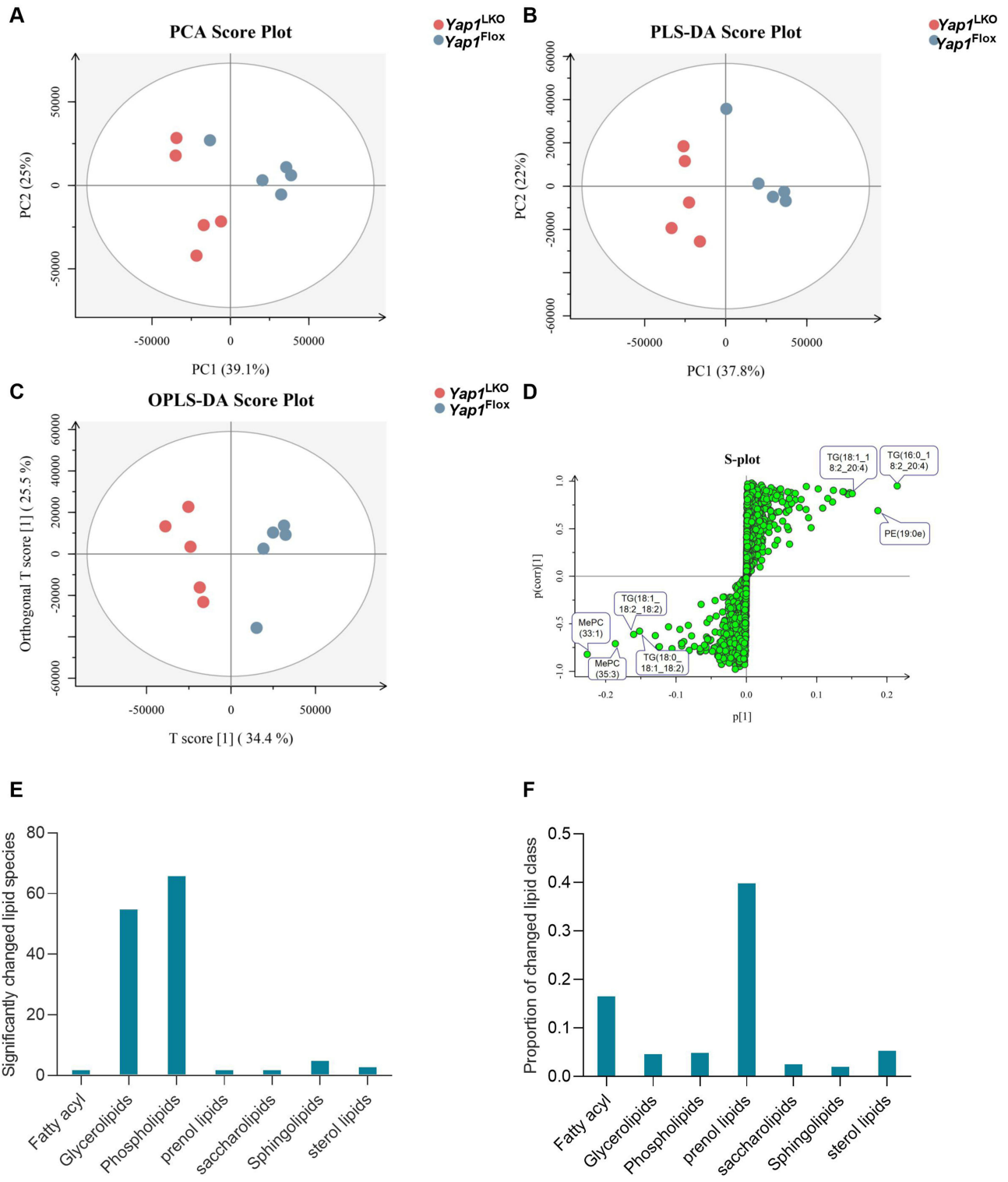

Figure 4 Multivariate statistical analysis was used to analyze the lipidomics data, the differences in lipid components between the two groups were verified by several analytical methods. (**A**) Principal Component Analysis (PCA) showed the lipid fractions of the two groups. The degree of aggregation and dispersion of samples can be observed from PCA score chart. (**B**) Least Squares-Discriminant Analysis (PLS-DA) showed the lipid fractions of the two groups. (**C**) Orthogonal Partial Least Squares Discriminant Analysis (OPLS-DA) showed the lipid fractions of the two groups. (**D**) OPLS-DA loading plot. P value≤0.05 and OPLS-DA first principal component variable importance value projection (VIP)≥1. (**E**) The number of lipid molecules that vary in each lipid class. (**F**) The percentage of lipid molecules that vary in each lipid class as measured in that class.

(CerG2GNAc1); and saccharolipids, including digalactosyldiacylglycero (DGDG), and sulfoquinovosyldiacylglycerol (SQDG) (Figure 5A). We plotted the percentages to illustrate better the proportion of the changed lipid subclasses in the detected lipids (Figure 5B). For example, the most significant number of TG molecules changed because the largest number of TG molecules were detected. When the ratio for the changed number to the detected number was calculated, the ratio was relatively low. In order to better elucidate the proportion of each lipid subclass in the 135 lipid molecules with significant changes, a pie chart was drawn (Figure 5C). Compared with the *Yap1*^{Flox} group, the changes of 135 lipid molecules were either increased or decreased in the *Yap1*^{LKO} group (Figure 5D). The increased percentage of lipid molecules was shown in red, and the decrease was in blue. The other lipid subclasses were all decreased except for MePc, CmE, ZyE, PC, PE, PI and SM, the other lipid subclasses decreased. The results indicated that *Yap1*^{LKO} effectively changed phospholipids, glycerolipids, prenol lipids, sterol lipids, saccharolipids sphingolipids, and fatty acyls metabolisms.

Yap1^{LKO} Effect on 135 Lipid Molecules

The Z-score was calculated based on the mean and standard deviation of the reference data set (control group) using the formula $Z = (x-\mu)/\sigma$. Where x is a specific fraction, μ is the mean, and σ is the standard deviation (Figure 6A). We use agglomerate hierarchical clustering to analyze the relationship between the components: grouping each object into a class and merging these classes into larger and larger objects until termination. The data set was scaled by the heat map program package in R (V3.3.2). Meanwhile, the hierarchical cluster diagram of relative quantitative lipid values was as follows. The size of relative contents was displayed by different colors, where columns represented samples and rows represented lipids (Figure 6B). The heat map showed that the differences were minor in lipids within the groups while the differences were significant between the groups. These results suggested that *Yap1*^{LKO} had a greater impact on lipids.

Lipid Components Interacted with Each Other

In order to show the relationship between various lipids more visually, we drew the Chord Diagram (Figure 7A). Many lines connected each lipid subclass through the Chord Diagram, suggesting that the lipids were related to each other. As for the relationship between each lipid component, the correlation map was drawn (Figure 7B). Positive and negative correlations were shown in different colors, with positive correlations in red and negative correlations in blue. The depth of the color indicated the degree of relevance, and the darker the color, the greater the degree of relevance. These results showed that there were apparent correlations among lipid components. *Yap1*^{LKO} improved lipid disorder induced by AAI combined with CCL_4.

Triglyceride Level in the Liver was Decreased on *Yap1*^{LKO} Mice

The expression of YAP1 and PLIN2 in *Yap1*^{LKO} mice was weaker than in *Yap1*^{Flox} group by immunohistochemistry (Figure 8A). Lipid levels in the liver were also measured, given the decrease in serum triglyceride levels and the altered liver lipidomics. Liver glucose levels did not change significantly after AAI+CCL_4, and there was no significant difference between *Yap1*^{LKO} and *Yap1*^{Flox} group ($P>0.05$) (Figure 8B). Liver cholesterol levels did not change significantly after AAI+CCL_4, and there was no significant difference between *Yap1*^{LKO} and *Yap1*^{Flox} group (Figure 8C) ($P>0.05$). In contrast, the hepatic triglyceride level was significantly increased after AAI+CCL_4, while the *Yap1*^{LKO} group compared with the *Yap1*^{Flox} group (Figure 8D) was significantly decreased ($P<0.05$). These results indicated that *Yap1*^{LKO} reduced hepatic PLIN2 expression and hepatic triglyceride levels in AAI+CCL_4 induced mice.

Triglyceride Level in the Liver was Decreased in *Yap1*^{LKO} Mice

To further explore the effect of *Yap1*^{LKO} on the liver of HFD-fed mice, we used 8-week-old mice for experiments (Figure 9A). Serum metabolic indexes showed no significant difference in glucose and cholesterol between the *Yap1*^{LKO} and *Yap1*^{Flox} group (Figure 9B) ($P > 0.05$). Triglyceride level decreased significantly compared with the *Yap1*^{Flox} group, and the difference was statistically significant (Figure 9B) ($P<0.05$). There was no significant difference in serum glucose and cholesterol between the *Yap1*^{LKO} and *Yap1*^{Flox} group (Figure 9C) ($P > 0.05$). Liver triglyceride levels decreased significantly compared with the *Yap1*^{Flox} group, and the difference was statistically significant (Figure 9C) ($P<0.05$).

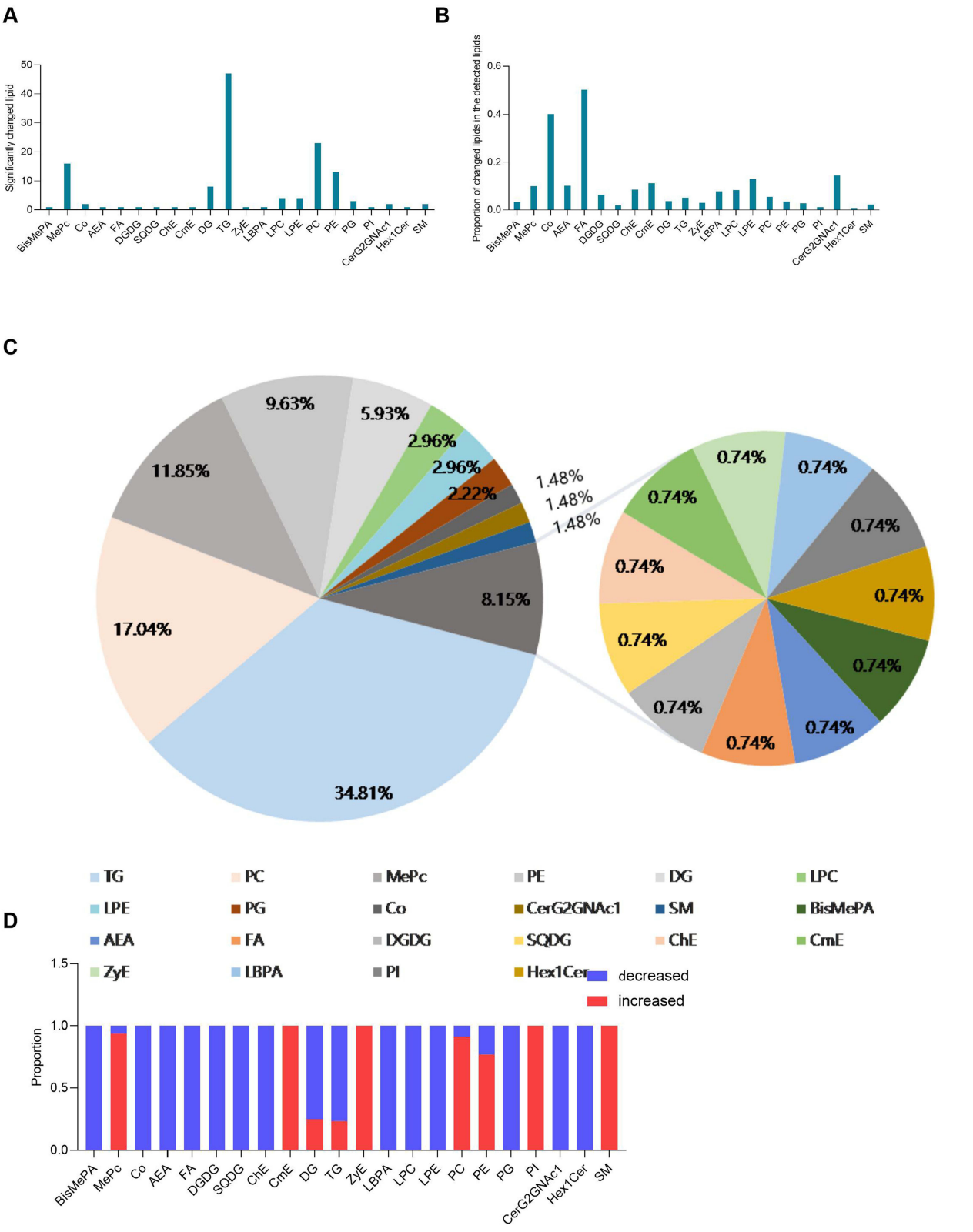

Figure 5 Lipid classification of *Yap1*^{LKO} group compared with *Yap1*^{Flox} group. (**A**) The number of lipid molecules that vary in each lipid subclass. (**B**) The percentage of lipid molecules measured in the lipid subclass that vary in each lipid class. (**C**) The percentage of altered lipid molecules in each lipid subclass. (**D**) The changes of lipid molecules in each lipid subclass.

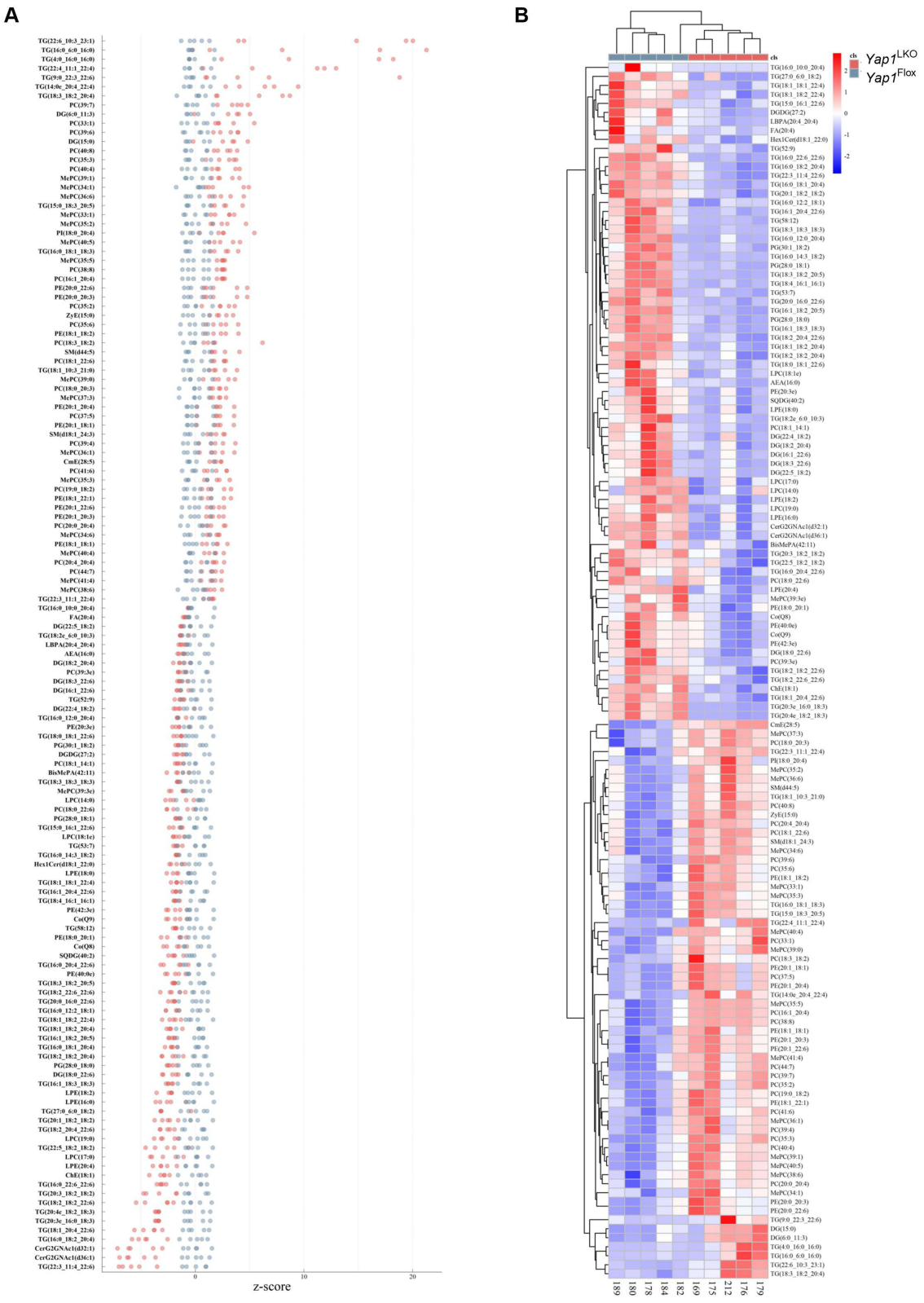

Figure 6 Lipid classification of *Yap1*^{LKO} group compared with *Yap1*^{Flox} group. (**A**) Standard score chart was converted according to the relative lipid content and used to measure the relative lipid content at the same level. (**B**) Differential lipid heat map.

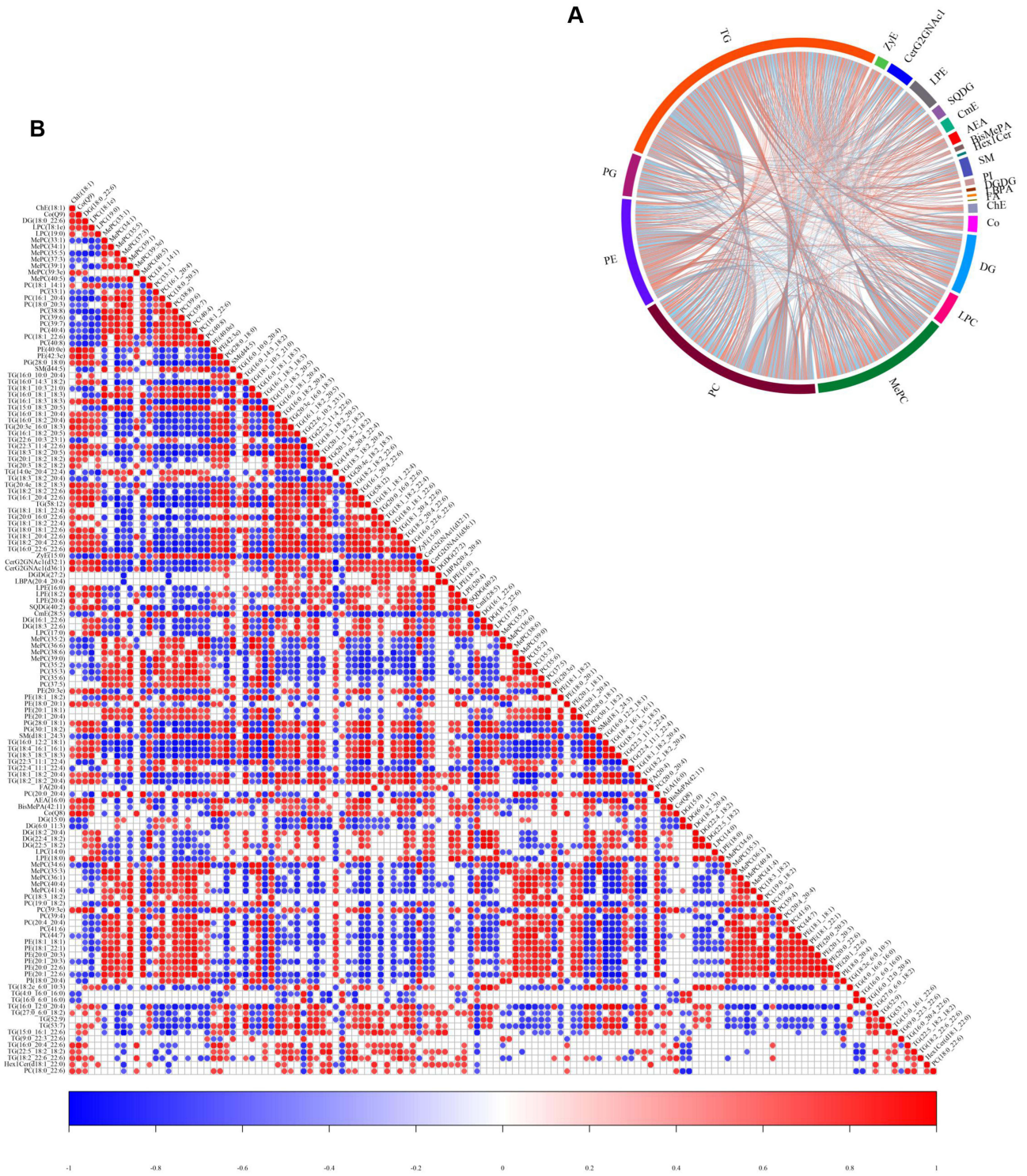

Figure 7 Lipid relationship diagram. (**A**) Differential lipid association chord chart. (**B**) Differential lipid-associated heat map. When the linear relationship between two lipids was enhanced, the correlation coefficient tended to 1 or −1: positive correlation tended to 1, negative correlation tended to −1. At the same time, cor.test function in R (V3.1.3) was used for statistical test of lipid association analysis, P value<0.05 was significantly correlated.

Liver vacuolization was significantly reduced in the *Yap1*^{LKO} group by H&E staining (Figure 9D). The expression of PLIN2 in *Yap1*^{LKO} mice was weaker than in the *Yap1*^{Flox} group by immunohistochemistry (Figure 9D). The results showed that *Yap1*^{LKO} reduced serum and hepatic triglyceride levels and reduced hepatic vacuolar degeneration and hepatic PLIN2 expression in HFD mice.

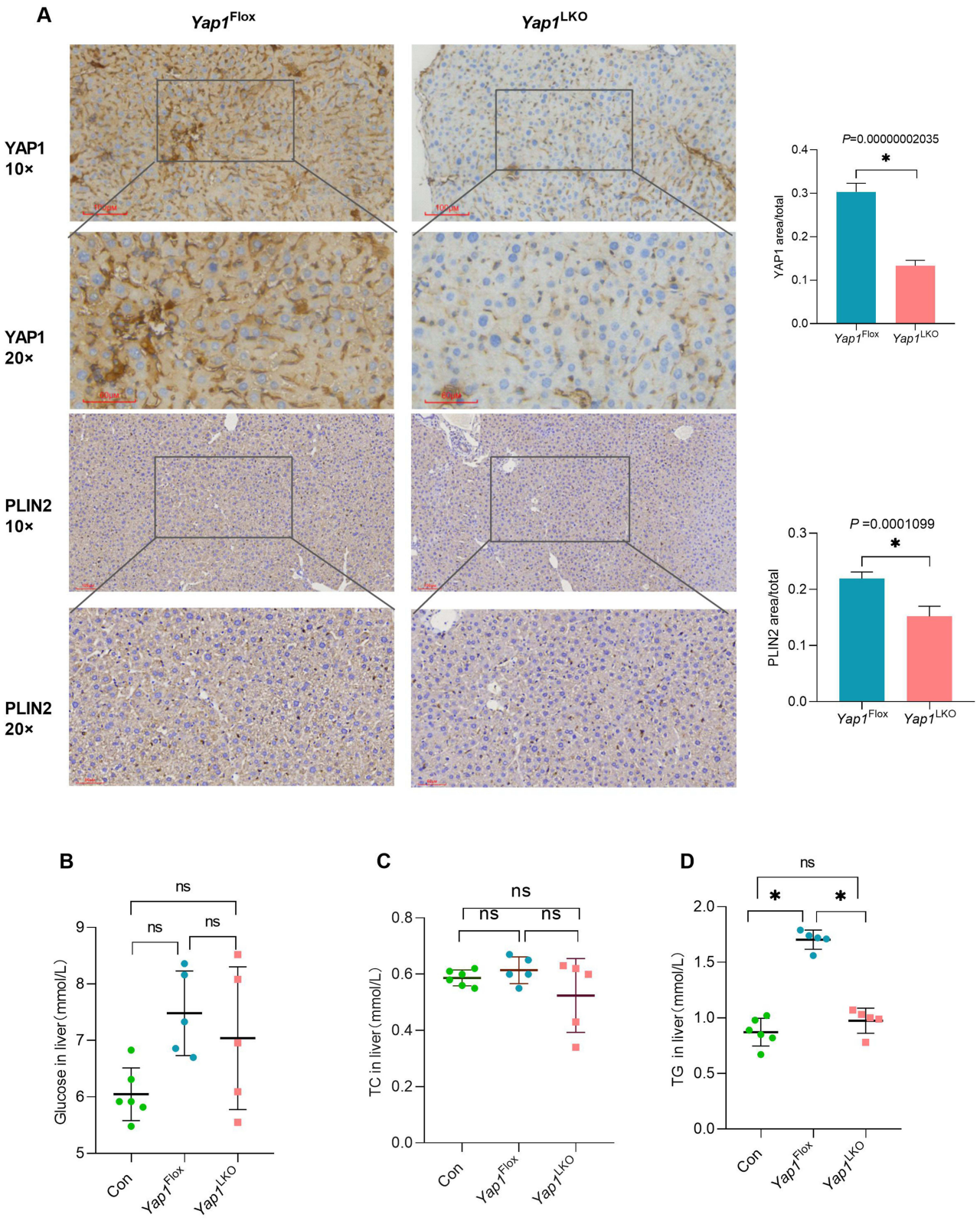

Figure 8 Immunohistochemical staining and biochemical indices of liver. (**A**) Liver immunohistochemical staining for YAP1 and PLIN2. (**B**) Liver glucose was not statistically different among the three groups. (**C**) Liver cholesterol was not statistically different among the three groups. (**D**) The liver triglyceride level was significantly increased after AAI+CCL_4, while the *Yap1*^{LKO} group compared with the *Yap1*^{Flox} group was significantly decreased. * P<0.05. n≥5.

https://doi.org/10.2147/DMSO.S472778 DovePress

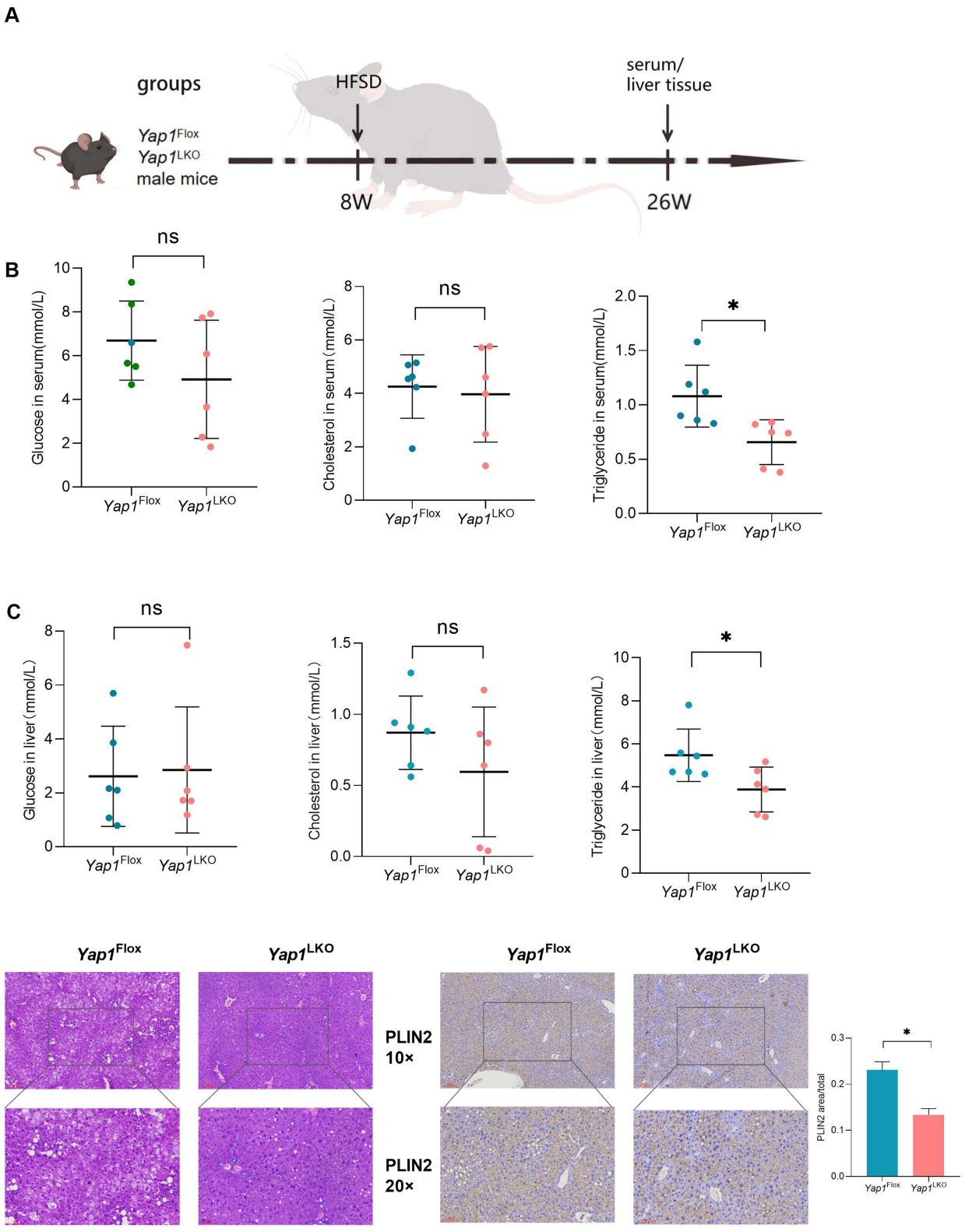

Figure 9 Liver pathology and biochemistry of *Yap1*^{LKO} in high-fat fed mice. (**A**) The model of high-fat fed mice. (**B**) Serum biochemical parameter. *Yap1*^{LKO} triglyceride decreased. (**C**) Liver biochemical parameter. *Yap1*^{LKO} triglyceride decreased. (**D**) Liver pathology and Immunohistochemical of PLIN2. Liver vacuolization was significantly reduced in the *Yap1*^{LKO} group. PLIN2 in *Yap1*^{LKO} mice was weaker than in the *Yap1*^{Flox} group. * P<0.05. n≥5.

Discussion

Nonalcoholic fatty liver disease (NAFLD) is the leading cause of chronic liver disease worldwide, with a global prevalence of 25%.[22] Gypenosides (GP) can regulate the key genes involved in hepatic lipid metabolism in NAFLD mice, providing initial evidence for the mechanisms underlying the therapeutic effect of GP in NAFLD.[23] The metabolites associated with poor clinical prognosis in patients with NAFLD combined with coronary artery disease include increased aristolochic acid compared with NAFLD alone.[13] Aristolochic acid is widely found in the genera Aristolochia and Asarum, and it belongs to the carboxylic acid group. Analysis of publicly available data suggests widespread AA exposure in self-identified Asian populations in East and Southeast Asia and elsewhere. At the same time, mutations in AA signatures have been proposed as cancer drivers, and animal studies suggest that mutations in AA adducts and possibly AA signatures occur in the liver.[24] AAI promoted clonal expansion only in the high-dose group but did not induce nodules or hepatocellular carcinoma in the adult rat liver.[25] There was a significant dose-dependent relationship between aristolochic acid intake and hepatocellular carcinoma (HCC) in patients with hepatitis virus infection.[26,27] In mice without hepatitis virus infection, AAI alone induced HCC in a dose-dependent manner. At the same time, the combination of AAI with CCl_4 led to a higher incidence of HCC in mice, and low-dose AAI combined with CCL_4 could induce hepatocellular carcinoma in mice starting at 2 weeks of age.[17] In the natural environment, a variety of inflammatory substances are widely present. After the body has been exposed to aristolochic acid, intermittent exposure to inflammatory substances will lead to the aggravation of the body's damage and then induce tumors. We used a small dose of AAI combined with CCL_4 administration and did not find clear liver tumors in mice at 26 weeks of age. No tumor cells were found in the liver of *Yap1*^{LKO} mice or *Yap1*^{Flox} mice. Increased liver LD were observed in *Yap1*^{Flox} mice, while reduced liver LD were observed in *Yap1*^{LKO} mice. Analysis of the reason may be that the intervention time was relatively late compared with our mice. The 2-week-old mice were still in the lactation period, and the liver and kidney functions of the 3-week-old mice were relatively more perfect. Lactating infants are generally not exposed to substances containing aristolochic acid, and when the liver function is relatively perfect, exposure to substances containing aristolochic acid will no longer cause hepatocellular carcinoma.

AAI can increase liver weight, serum AST and Alt levels, hepatocyte swelling, vesicular degeneration, and steatosis in Tianfu broilers.[28] Another study in rats found diffuse liver tissue swelling with hepatocyte vacuolar degeneration in the AAI group. In the AAI group, 33 serum lipids were changed, and 18 lipid changes were found in the liver. According to histological characteristics, serum biochemical indicators, and lipidomics characteristics, AAI-induced hepatotoxicity was reversible. The characteristic pathological changes of the liver are often accompanied by the disorder of lipid homeostasis.[29] Our study found that AAI + CCL_4 caused diffuse swelling of liver tissue, increased vacuolar degeneration of hepatocytes, and elevated serum triglycerides, indicating that AAI + CCL_4 led to increased lipid droplet deposition in the liver.

YAP1, the downstream effector of Hippo signaling, is involved in many cellular and non-cell autonomous functions, such as the interaction between metabolism and the immune system. The regulation and biological functions of Hippo signaling are often organ or even cell-type-specific.[30] The research on YAP1 mainly focuses on tumors, and the research on YAP1 and metabolism has also attracted attention in recent years. Some studies have investigated the effect of metformin on the growth and viability of melanoma cells cultured in vitro and found that metformin significantly reduced the expression of YAP1 and enhanced YAP1 phosphorylation.[31] Oil red O staining showed that the area of LD and the expression of PLIN2 in sh*YAP1*-HepG2215 cells were also reduced in *YAP1*-knockdown HepG2215 cells.[6] However, the relationship between liver metabolism and YAP1 has yet to be elucidated in the liver induced by AAI+CCL_4. This study found that AAI+CCL_4 led to lipid metabolism disorders, but hepatocyte-specific *Yap1* knockout improved this imbalance. From the metabolomics perspective, the possible mechanism was that knockout of hepatocyte *Yap1* reduced LD deposition and TG content, but not cholesterol content, without affecting glucose metabolism in the liver. Inhibition of YAP1 activity ameliorated hepatic steatosis when there was no significant change in liver function indicators, which had specific clinical value.

A study found that lipomics was used to study the hepatotoxicity mechanism of AAI. The results showed that 26 lipid markers were observed in rat serum and liver, of which 9 kinds of lipids had high sensitivity and specificity, which could

be the difference between the administration and the control group. These changed lipid markers indicated that AAI led to the occurrence of hepatotoxicity and its mechanism of action.[29] The changes in lipid markers were closely related to histopathological and biochemical abnormalities in the liver. TG was a substance formed by the esterification of glycerol and FAs. It was the most abundant lipid in the mammalian body, serving as a storage and transport agent.[32] In this study, AAI+CCL_4-induced liver vacuolation and LD deposition in *Yap1*^{Flox} mice. Similarly, CCL_4 increased hepatic TG levels, which caused its accumulation in the liver, leading to hepatomegaly.[33] Moreover, TG content was significantly increased after AAI treatment in the serum.[12] This study also found that YAP1 knockout reduced liver vacuolation, TG content, 36 TG-associated lipid molecules, and PLIN2 expression in AAI+CCL_4-induced mice. Moreover, different lipid molecules interacted with each other, and TG-related lipids affected the expression of PE and PC.

Lipids are not only the significant constituents of the cell membrane and very efficient energy sources but also key pathophysiological mediators of intracellular and extracellular processes. The liver is the main organ of FAs oxidation and ketone body formation. The characteristic pathological changes of the liver were often accompanied by disturbance of lipid homeostasis.[29] Studies showed that liver injury increased lipid synthesis in the liver, reduced the β-oxidation capacity of FAs, and interfered with the thyroid hormone pathway, affecting lipid metabolism.[34] Phospholipids were divided into glycerophospholipids and sphingomyelins. Phospholipid abnormality was closely related to liver failure.[35] Phospholipids composed of glycerol were called glycerophospholipids. PE and PC were two essential compounds in glycerophospholipids.[36] The ratio of PC: PE was a key regulator in cell membrane integrity.[37] Lipid metabolism disorders, such as PC and PE, led to variations in membrane lipid composition, which affected the physical properties and integrity of the membrane, leading to inflammation and liver disease progression.[38] Moreover, PC deficiency leads to impaired DNA methylation and self-repair in liver cells, damaging liver cells.[39] The contents of PC and PE were decreased, and the ratio of PE: PC increased in CCL_4-induced liver injury in rats.[40] Moreover, in the remodeling of PC/PE, the FA composition of PC changed, and PE decreased in rats with liver injury induced by Tripterygium wilfordii.[41] After AAI treatment, various lipids were decreased in both liver and serum samples, such as PC and PE.[29] In this study, we found that *Yap1*^{LKO} upregulated 20 PC-related lipids and 9 PE-related lipids. These results showed that *Yap1*^{LKO} played a role in liver protection by regulating glycerol phospholipid metabolism and TG metabolism disorder.

YAP1 was the main effector of the Hippo pathway and involved in metabolic regulation, such as fat production.[42] Our study found that hepatocyte-specific *Yap1* knockout reduced TG and LD, but not cholesterol, without affecting glucose metabolism. Moreover, studies also showed that YAP1 was increased and was highly correlated with liver injury in nonalcoholic fatty liver disease.[8] YAP1 overexpression in white adipose tissue induces fat mass increases.[43] Besides, studies showed that YAP1 levels were elevated in the livers of monkeys with non-alcoholic fatty liver disease, and YAP1 in both simple fatty livers and at fibrosis stage 1a were significantly lower than in the standard group.[8] Adipocyte-specific YAP1 deficiency leads to increased adipocyte death during obesity.[44] We found that *Yap1*^{LKO} reduced TG levels, decreased PLIN2 expression level, and alleviated hepatic vacuolar degeneration in mice. These results further demonstrated that the abnormal expression of YAP1 was closely related to lipid metabolism disorder.

Conclusion

In summary, *Yap1*^{LKO} reduced liver LD in mice induced by AAI + CCL_4 and HFD, which laid a theoretical foundation for the clinical application of YAP1 inhibitors to ameliorate LD deposition in liver disease. Moreover, *Yap1*^{LKO} mainly reduced TG and upregulated PC-related and PE-related lipids in the liver, but did not affect cholesterol or glucose metabolism, leading to improving lipid metabolism disorders, which had a potential role in metabolism-related liver disease. Therefore, YAP1 expression was associated with lipid metabolism, and maintained lipid metabolism homeostasis and protected the liver under long-term damage stimulation. However, further experiments are needed to explore the pathway by which YAP1 affects lipid metabolism.

Data Sharing Statement

The datasets used and/or analyzed during the current study are available from the corresponding author on reasonable request.

Acknowledgments

This work was financially supported by the National Natural Science Foundation of China (82274315), Hebei Graduate Innovation Funding Project (XCXZZBS2022005), and Medical Science Research Project of Hebei Province (20210507).

Disclosure

The authors declare no conflicts of interest in this work.

References

1. Dong J, Feldmann G, Huang J, et al. Elucidation of a universal size-control mechanism in Drosophila and mammals. *Cell*. 2007;130(6):1120–1133. doi:10.1016/j.cell.2007.07.019
2. Piccolo S, Dupont S, Cordenonsi M. The biology of YAP/TAZ: hippo signaling and beyond. *Physiol Rev*. 2014;94(4):1287–1312.
3. Zheng Y, Pan D. Zheng Y and Pan D The Hippo Signaling Pathway in Development and Disease. *Dev Cell*. 2019;50(3):264–282. doi:10.1016/j.devcel.2019.06.003
4. Shu Z, Gao Y, Zhang G, et al. A functional interaction between Hippo-YAP signalling and SREBPs mediates hepatic steatosis in diabetic mice. *J Cell Mol Med*. 2019;23(5):3616–3628. doi:10.1111/jcmm.14262
5. Wang L, Wang S, Shi Y, et al. YAP and TAZ protect against white adipocyte cell death during obesity. *Nat Commun*. 2020;11(1):5455. doi:10.1038/s41467-020-19229-3
6. Hao L, Guo Y, Peng Q, et al. Dihydroartemisinin reduced lipid droplet deposition by YAP1 to promote the anti-PD-1 effect in hepatocellular carcinoma. *Phytomedicine*. 2022;96:153913. doi:10.1016/j.phymed.2021.153913
7. Cruz ALS, Barreto EA, Fazolini NPB, et al. Lipid droplets: platforms with multiple functions in cancer hallmarks. *Cell Death Dis*. 2020;11(2):105. doi:10.1038/s41419-020-2297-3
8. Chen P, Luo Q, Huang C, et al. Pathogenesis of non-alcoholic fatty liver disease mediated by YAP. *Hepatol Int*. 2018;12(1):26–36. doi:10.1007/s12072-017-9841-y
9. Mcmanaman JL, Bales ES, Orlicky DJ, et al. Perilipin-2-null mice are protected against diet-induced obesity, adipose inflammation, and fatty liver disease. *J Lipid Res*. 2013;54(5):1346–1359.
10. Hu SL, Zhang HQ, Chan K, et al. Studies on the toxicity of Aristolochia manshuriensis (Guanmuton). *Toxicology*. 2004;198(1–3):195–201. doi:10.1016/j.tox.2004.01.026
11. Li J, Zhang L, Jiang Z, et al. Toxicities of aristolochic acid I and aristololactam I in cultured renal epithelial cells. *Toxicol In Vitro*. 2010;24(4):1092–1097. doi:10.1016/j.tiv.2010.03.012
12. Wang Z, He B, Liu Y, et al. In situ metabolomics in nephrotoxicity of aristolochic acids based on air flow-assisted desorption electrospray ionization mass spectrometry imaging. *Acta Pharm Sin B*. 2020;10(6):1083–1093. doi:10.1016/j.apsb.2019.12.004
13. Hu X, Zhou R, Li H, et al. Alterations of Gut Microbiome and Serum Metabolome in Coronary Artery Disease Patients Complicated With Non-alcoholic Fatty Liver Disease Are Associated With Adverse Cardiovascular Outcomes. *Front Cardiovasc Med*. 2021;8:805812. doi:10.3389/fcvm.2021.805812
14. Ali S, Khan MR, Sajid M. Protective potential of Parrotiopsis jacquemontiana (Decne) Rehder on carbon tetrachloride induced hepatotoxicity in experimental rats. *Biomed Pharmacother*. 2017;95:1853–1867. doi:10.1016/j.biopha.2017.09.003
15. Ali S, Khan MR, Shah SA, et al. Protective aptitude of Periploca hydaspidis Falc against CCl(4) induced hepatotoxicity in experimental rats. *Biomed Pharmacother*. 2018;105:1117–1132. doi:10.1016/j.biopha.2018.06.039
16. Ishikawa M, Saito K, Yamada H, et al. Plasma lipid profiling of different types of hepatic fibrosis induced by carbon tetrachloride and lomustine in rats. *Lipids Health Dis*. 2016;15(1). doi:10.1186/s12944-016-0244-1.
17. Lu ZN, Luo Q, Zhao LN, et al. The Mutational Features of Aristolochic Acid-Induced Mouse and Human Liver Cancers. *Hepatology*. 2020;71(3):929–942. doi:10.1002/hep.30863
18. Van Meer G, Voelker DR, Feigenson GW. Membrane lipids: where they are and how they behave. *Nat Rev Mol Cell Biol*. 2008;9(2):112–124. doi:10.1038/nrm2330
19. Rolim AE, Henrique-Araujo R, Ferraz EG, et al. Lipidomics in the study of lipid metabolism: current perspectives in the omic sciences. *Gene*. 2015;554(2):131–139. doi:10.1016/j.gene.2014.10.039
20. Griffiths WJ, Ogundare M, Williams CM, et al. On the future of "omics": lipidomics. *J Inherit Metab Dis*. 2011;34(3):583–592. doi:10.1007/s10545-010-9274-4
21. Zheng K, Zhou W, Ji J, et al. Si-Ni-San reduces lipid droplet deposition associated with decreased YAP1 in metabolic dysfunction–associated fatty liver disease. *J Ethnopharmacol*. 2023;305:116081.
22. Lazarus JV, Mark HE, Anstee QM, et al. Advancing the global public health agenda for NAFLD: a consensus statement. *Nat Rev Gastroenterol Hepatol*. 2021;19(1):60–78.
23. Zhou T, Cao L, Du Y, et al. Gypenosides ameliorate high-fat diet-induced nonalcoholic fatty liver disease in mice by regulating lipid metabolism. *PeerJ*. 2023;11: e15225.
24. Ng AWT, Poon SL, Huang MN, et al. Aristolochic acids and their derivatives are widely implicated in liver cancers in Taiwan and throughout Asia. *Sci Trans Med*. 2017;9(412). doi:10.1126/scitranslmed.aan6446.
25. Liu YZ, Lu HL, Qi XM, et al. Aristolochic acid I promoted clonal expansion but did not induce hepatocellular carcinoma in adult rats. *Acta Pharmacol Sin*. 2021;42(12):2094–2105. doi:10.1038/s41401-021-00622-7
26. Chen CJ, Yang YH, Lin MH, et al. Herbal medicine containing aristolochic acid and the risk of hepatocellular carcinoma in patients with hepatitis B virus infection. *Int J Cancer*. 2018;143(7):1578–1587. doi:10.1002/ijc.31544
27. Chen CJ, Yang YH, Lin MH, et al. Herbal Medicine Containing Aristolochic Acid and the Risk of Primary Liver Cancer in Patients with Hepatitis C Virus Infection. *Cancer Epidemiol Biomarkers Prev*. 2019;28(11):1876–1883. doi:10.1158/1055-9965.EPI-19-0023

28. Xu D, Yin L, Lin J, et al. Aristolochic Acid I-Induced Hepatotoxicity in Tianfu Broilers Is Associated with Oxidative-Stress-Mediated Apoptosis and Mitochondrial Damage. *Animals*. 2021;11(12):3437.
29. Zhou J, Yang Y, Wang H, et al. The Disturbance of Hepatic and Serous Lipids in Aristolochic Acid Iota Induced Rats for Hepatotoxicity Using Lipidomics Approach. *Molecules*. 2019;24(20):3745.
30. Du X, Wen J, Wang Y, et al. Hippo/Mst signalling couples metabolic state and immune function of CD8alpha(+) dendritic cells. *Nature*. 2018;558 (7708):141–145. doi:10.1038/s41586-018-0177-0
31. Lee GJ, Kim YJ, Park B, et al. YAP-dependent Wnt5a induction in hypertrophic adipocytes restrains adiposity. *Cell Death Dis*. 2022;13(4):407. doi:10.1038/s41419-022-04847-0
32. Mcalpin CR, Voorhees KJ, Corpuz AR, et al. Analysis of lipids: metal oxide laser ionization mass spectrometry. *Anal Chem*. 2012;84 (18):7677–7683. doi:10.1021/ac300688u
33. K-H L, Weng C-Y, Chen W-C, et al. Ginseng essence, a medicinal and edible herbal formulation, ameliorates carbon tetrachloride-induced oxidative stress and liver injury in rats. *J Ginseng Res*. 2017;41(3):316–325. doi:10.1016/j.jgr.2016.06.002
34. Wu C, Zhang Y, Chai L, et al. Histological changes, lipid metabolism and oxidative stress in the liver of Bufo gargarizans exposed to cadmium concentrations. *Chemosphere*. 2017;179:337–346. doi:10.1016/j.chemosphere.2017.03.131
35. Ming YN, Zhang JY, Wang XL, et al. Liquid chromatography mass spectrometry-based profiling of phosphatidylcholine and phosphatidylethanolamine in the plasma and liver of Acetaminophen-induced liver injured mice. *Lipids Health Dis*. 2017;16(1):153. doi:10.1186/s12944-017-0540-4
36. O'donnell VB, Rossjohn J, Wakelam MJO. Phospholipid signaling in innate immune cells. *J Clin Investig*. 2018;128(7):2670–2679. doi:10.1172/JCI97944
37. Escriba PV, Gonzalez-Ros JM, Goni FM, et al. Membranes: a meeting point for lipids, proteins and therapies. *J Cell Mol Med*. 2008;12(3):829–875. doi:10.1111/j.1582-4934.2008.00281.x
38. Payne F, Lim K, Girousse A, et al. Mutations disrupting the Kennedy phosphatidylcholine pathway in humans with congenital lipodystrophy and fatty liver disease. *Proc Natl Acad Sci U S A*. 2014;111(24):8901–8906.
39. Chamulitrat W, Burhenne J, Rehlen T, et al. Bile salt-phospholipid conjugate ursodeoxycholyl lysophosphatidylethanolamide as a hepatoprotective agent. *Hepatology*. 2009;50(1):143–154.
40. Shimizu Y. Effect of carbon tetrachloride administration on the synthesis of triglycerides and phospholipids in rat liver. *J Lipid Res*. 1969;10 (5):479–486.
41. Xie T, Zhou X, Wang S, et al. Development and application of a comprehensive lipidomic analysis to investigate Tripterygium wilfordii-induced liver injury. *Anal Bioanal Chem*. 2016;408(16):4341–4355. doi:10.1007/s00216-016-9533-9
42. Koo JH, Guan KL. Interplay between YAP/TAZ and Metabolism. *Cell Metab*. 2018;28(2):196–206. doi:10.1016/j.cmet.2018.07.010
43. Kamura K, Shin J, Kiyonari H, et al. Obesity in Yap transgenic mice is associated with TAZ downregulation. *Biochem Biophys Res Commun*. 2018;505(3):951–957. doi:10.1016/j.bbrc.2018.10.037
44. Zhu C, Tabas I, Schwabe RF, et al. Maladaptive regeneration - The reawakening of developmental pathways in NASH and fibrosis. *Nat Rev Gastroenterol Hepatol*. 2021;18(2):131–142. doi:10.1038/s41575-020-00365-6